Journal of
Materials Chemistry B

Materials for biology and medicine

www.rsc.org/MaterialsB

ROYAL SOCIETY
OF CHEMISTRY

PAPER

Core–shell clusters of human haemoglobin A and human serum albumin: artificial O2-carriers having various O2-affinities†

Takuya Kimura,[a] Ryuichi Shinohara,[a] Christoph Böttcher[b] and Teruyuki Komatsu*[a]

This report describes the synthesis, structure, and O2-binding properties of core–shell clusters composed of human haemoglobin A (HbA) in the centre and human serum albumin (HSA) at the periphery (HbA–HSA$_m$) as potential O2-carriers designed as red blood cell (RBC) substitutes. Protein clusters were prepared by covalent linkages between HbA lysins and HSA cysteine-34 using a heterobifunctional cross-linker, succinimidyl-4-(*N*-maleimidomethyl)cyclohexane-1-carboxylate. Major products (m = 2, 3, 4) were isolated using gel filtration chromatography. The low isoelectric points (pI = 5.0–5.2) of the clusters were almost identical to that of HSA, proving the wrapping of HbA by negatively charged HSA. The 3D reconstruction of HbA–HSA$_3$ based on transmission electron microscopy images revealed a complete triangular structure. The proposed geometries enabled us to assign a possible spatial arrangement of the HbA centre and HSA periphery. The HbA–HSA$_m$ clusters showed higher O2-affinities (P_{50} = 8–9 Torr) than the native HbA. The clusters prepared under N2 atmosphere showed a low O2-affinity (P_{50} = 26 Torr) resembling those of human RBC. Moreover, the cluster containing an αα-cross-linked HbA with bis(3,5-dibromo-salicyl)fumarate showed a markedly low O2-affinity (P_{50} = 35 Torr). These HbA–HSA$_m$ clusters with various O2-affinities can support a new generation of RBC substitutes, which can be better tuned to play a role in O2 transport.

1. Introduction

Over the last 30 years, haemoglobin (Hb)-based O2 carriers (HBOCs) of several kinds have been prepared and evaluated as red blood cell (RBC) substitutes,[1–4] such as polymerized Hb,[5–7] poly(ethyleneglycol)-conjugated Hb,[8–10] enzyme-linked Hb,[11,12] and saccharide-bound Hb.[13] Nevertheless, because of several concerns, none has been assigned yet for practical use.[14,15] The first issue is vasoconstriction, which is observed for some materials and which causes a mild increase in blood pressure. Many researchers have inferred that the vasopressor response is attributable to rapid scavenging of the endothelial-derived relaxing factor, nitric oxide (NO), by Hb leaked into the extravascular space.[16–18] Lemon *et al.* reported that recombinant Hb

mutants (rHb) having low NO-association rates elicited a less hypertensive action than native Hb did.[17] The second concern is unmodulated O2-affinity. In general, cell-free HBOCs show individual and high O2-affinity compared to RBC.[6,9,10,13] High O2-affinity is thought to prevent the delivery of a sufficient amount of O2 to tissues under normal physiological conditions. In contrast, high O2-affinity avoids early O2 offloading on the arterial side of circulation and this is expected to be beneficial for targeted O2 transport to the hypoxic regions.[8,18] If one were able to create a novel cell-free HBOC with controllable O2-binding capability, then it might become a promising RBC substitute and an O2-providing therapeutic reagent that can be useful for clinical situations.

We previously demonstrated that covalent wrapping of bovine Hb (HbBv) using human serum albumin (HSA) generated a core–shell structured protein cluster, HbBv–HSA$_m$, as a unique HBOC.[19–21] Actually, HSA is a versatile protein (4–5 g dL^{-1}) in blood plasma. It shows low permeability in the vasculature walls attributable to the electrostatic repulsion between negatively charged albumin surfaces and the glomerular membrane.[22,23] Therefore, intravenous transfusion of the HbBv–HSA$_m$ cluster would not incite unfavourable vasoactivity because it might not extravasate through the vasculature. To develop this O2-carrying plasma protein as an alternative material for RBC transfusion in

[a] *Department of Applied Chemistry, Faculty of Science and Engineering, Chuo University, 1-13-27 Kasuga, Bunkyo-ku, Tokyo 112-8551, Japan. E-mail: komatsu@kc.chuo-u.ac.jp*

[b] *Research Centre of Electron Microscopy, Institute of Chemistry and Biochemistry, Freie Universität Berlin, Fabeckstrasse 36a, 14195 Berlin, Germany*

† Electronic supplementary information (ESI) available: Experimental details, IEF profiles of HbA–HSA$_m$ clusters (Fig. S1), the spatial molecular view of HbA–HSA$_3$ clusters (Movie S1), the diameter and pI values of HbA–HSA$_m$ clusters (Table S1), and UV-Vis absorption spectral data of HbA–HSA$_m$ clusters (Table S2). See DOI: 10.1039/c5tb00540j

This journal is © The Royal Society of Chemistry 2015

J. Mater. Chem. B, 2015, 3, 6157–6164 | 6157

clinical uses, additional work must be done. (i) Human adult Hb (HbA) must be exploited as a core protein. Some differences exist between HbBv and HbA in terms of the amino acid sequence and O_2-binding property.[24] (ii) The O_2 affinity should be tuned to some degree for various medical applications. This report describes, for the first time ever, the synthesis of a series of core–shell clusters HbA–HSA_m, comprising HbA and HSA. The results show that the O_2 affinities of the clusters are governed by the conformational state of the HbA core [T-(tense) or R-(relaxed) state], which is locked in during the preparation process. Consequently, HbA–HSA_m clusters having various O_2-affinities (P_{50} = 8–35 Torr) have been produced.

2. Experimental section

2.1. Materials and apparatus

Succinimidyl-4-(N-maleimidomethyl)cyclohexane-1-carboxylate (SMCC) was purchased from Tokyo Chemical Industry Co. Ltd. Human serum albumin (HSA) was purchased from the Japan Blood Products Organization. Bis(3,5-dibromosalicyl)fumarate (DBBF) was purchased from LKT Laboratories Inc. L-Glycine was purchased from Wako Pure Chemical Industries Ltd. Inositol hexaphosphate (IHP) was purchased from Sigma-Aldrich Corp. Human adult Hb (HbA) was purified from red blood cell concentrates received from the Japanese Red Cross Society (see ESI†). Other chemicals of special grade were used without further purification unless otherwise noted. Water was deionized (18.2 MΩ cm) using water purification systems (Elix UV and Milli Q Reference; Millipore Corp.). Native-PAGE was performed using an electrophoresis power supply (EPS 301; GE Healthcare) using 5–12% polyacrylamide precast gradient gel (SuperSep Ace 5–12%; Wako Pure Chemical Industries Ltd). Isoelectric focusing (IEF) was done using an electrophoresis power supply (EPS 601; GE Healthcare) using a pH 3–10 IEF gel (Novex; Invitrogen Corp.). A GE Healthcare IEF calibration kit Broad pI (pH 3–10) was used for the protein marker. The voltage was raised gradually to 500 V for 2 h.

2.2. Synthesis of HbA–HSA_m clusters

A freshly prepared DMSO solution of SMCC (20 mM, 4.0 mL) was added dropwise to the pure carbonyl HbA solution (0.1 mM, 40 mL in phosphate buffered saline solution, PBS) in a round-bottom flask (100 mL volume). After stirring under dark conditions in CO atmosphere for 3 h at 25 °C, the reactant was loaded for gel filtration chromatography (GFC) using a Sephadex G25 (superfine) column to remove the unreacted cross-linker. The eluent of SMCC–HbA was concentrated to 40 mL (Vivaspin 20 ultrafilter, 10 kDa MWCO; Sartorius AG). The obtained SMCC–HbA (0.1 mM, 40 mL) was added gradually to the HSA solution (1.0 mM, 40 mL in PBS). The reactant was stirred under dark conditions for 14 h at 4 °C. A part of the reaction mixture was used for size-exclusion chromatography (SEC) on an HPLC system (LaChrom Elite; Hitachi High-Technologies Corp.) equipped with a column (Shodex Protein KW-803; Showa Denko K.K.) using phosphate buffered (PB) solution (50 mM, pH 7.4) as the mobile phase.

The elution curve showed new multiple peaks in the high molecular weight region. Native-PAGE also showed new bands above HSA. Then the resultant solution was subjected to GFC on an FPLC system (Äkta Prime Plus; GE Healthcare UK Ltd) equipped with a Superdex 200 pg (HiLoad 26/60; GE Healthcare UK Ltd) column using PB (50 mM, pH 7.4) as the running buffer. The eluent was monitored at 280 nm and fractionated. The fractions showing a single band in the native-PAGE were collected. Each component was checked again using SEC measurements. The total protein concentration was assayed using a protein assay kit (Pierce 660 nm; Thermo Fisher Scientific Inc.). The Hb concentration was assayed (Hb assay kit, Nescoat Hemokit-N; Alfresa Pharma Corp.). The cysteinyl thiol assay of HbA was conducted by reaction with 4,4′-dithio-pyridine coupled with the sulphydryl group to give 4-thio-pyridinone with absorption at 324 nm.[25] The procedure of the maleimide assay on SMCC–HbA is described in the ESI.†

2.3. Synthesis of HbA–HSA_3 clusters

The reaction mixture of SMCC–HbA and HSA obtained in the above experiment (Section 2.2) was subjected to GFC (Superdex 200 pg in XK50/60 column; GE Healthcare UK Ltd) using PBS as the running buffer. We collected all the cluster products except for the unreacted HSA. The collected yield was 85% based on HbA. The average HSA/HbA ratio of the harvested cluster mixture was 3.0 ± 0.2, which is indicated as HbA–HSA_3 with italicized subscript 3.

2.4. CD and DLS measurements

The circular dichroism (CD) spectra were measured using a spectropolarimeter (J-820; Jasco Corp.). The sample concentration was 0.2 μM in PBS. Quartz cuvettes with 10 mm thickness were used. The molecular sizes of the clusters were ascertained using dynamic light scattering (DLS) measurements (Zetasizer Nano; Malvern Instruments, Ltd) at 25 °C. The diameters were estimated by the number obtained from the particle size distribution. Aqueous solutions with a concentration of 2 mg mL^{-1} were prepared using Milli-Q water.

2.5. Measurements, image processing, and 3D reconstruction

The transmission electron microscopy (TEM) observations of the HbA–HSA_3 clusters were conducted according to our previously reported procedures.[19] Image processing (single-particle analysis) and 3D reconstruction of the clusters based on the TEM data were conducted using our previously described techniques.[19,26,27] In short, the images of individual molecules (total 1800 sections) corresponding to different spatial orientations of individual clusters were identified, extracted, aligned, and summed to yield class sum images with an enhanced signal-to-noise ratio (SNR). Automatic classification was conducted using the IMAGIC-5 software (Image Science Software GmbH, Berlin, Germany) and a multivariate statistical analysis (MSA) technique.[28] Angular reconstitution was used to assign the angular relationship between the obtained 'class averages' (Euler angles).[29] Further refinements were obtained using "anchor-set" reprojection images as references. No symmetry operation was used in the reconstruction.

6158 | J. Mater. Chem. B, 2015, 3, 6157–6164

This journal is © The Royal Society of Chemistry 2015

2.6. O_2-binding property

The visible absorption spectra were recorded using a UV-Visible spectrophotometer (8543; Agilent Technologies Inc.) equipped with a temperature control unit (89090A; Agilent Technologies Inc.). To prepare oxy HbA–HSA_m clusters, O_2 gas was flowed to PBS (pH 7.4) containing carbonyl HbA–HSA_m clusters ([Hb]: *ca.* 10 μM) in an optical quartz cuvette (10 mm path length) sealed with a rubber septum under light (500 W halogen lamp) in an ice-water bath. Next, N_2 gas was flowed continuously to the O_2 complex solution, yielding deoxy HbA–HSA_m. The O_2 affinity (P_{50}: O_2-partial pressure where Hb is half-saturated with O_2) and the Hill coefficient (n) were determined using an automatic recording system for blood O_2-equilibrium curves (Hemox Analyzer; TCS Scientific Corp.) using PBS (pH 7.4) at 37 °C. The sample was oxygenated under an increased O_2-partial pressure and deoxygenated by flushing with N_2.

2.7. Synthesis of HbA(T)–HSA_3 clusters under N_2 atmosphere

A DMSO solution of SMCC (20 mM, 0.5 mL) was added dropwise to the deoxy HbA solution (0.1 mM, 5 mL in PBS) under humidified N_2 atmosphere at 25 °C. Before the addition of SMCC, HbA must be fully deoxygenated. The mixture was stirred for 2 h and poured into the PBS solution of glycine (150 mM, 0.33 mL) using a humidified N_2 gas stream, followed by stirring for 1 h at 25 °C to quench the unreacted cross-linker. Then the reactant was added gradually into the HSA solution (2.0 mM, 10 mL in PBS) under N_2 gas pressure. It was stirred in the dark for 14 h at 25 °C. No further effort was made to exclude O_2 thereafter. A part of the reaction mixture was subjected to SEC on an HPLC system equipped with a column (Shodex Protein KW-803; Showa Denko K.K.) using PB (50 mM, pH 7.4) as the mobile phase. The elution curve showed multiple peaks in the high molecular weight region. Native-PAGE also revealed three bands above HSA. The resultant solution was subjected to GFC (Superdex 200 pg in XK50/60 column; GE Healthcare UK Ltd) using PBS (pH 7.4, 50 mM) as the running buffer. We collected all cluster products except for HSA. Using the total protein and Hb assays, the average HSA/HbA ratio of the harvested clusters was found to be 2.9 ± 0.2, which is indicated as HbA(T)–HSA_3.

2.8. Synthesis of ααHbA(T)–HSA_3 clusters under N_2 atmosphere

First, αα-cross-linked HbA(T) [ααHbA(T)] was prepared as described in a report by Walder *et al.*[30,31] The PBS solution (pH 7.2) of IHP (25 mM, 0.5 mL) was mixed with the oxy HbA solution (0.1 mM, 30 mL in PBS) in a round-bottom flask (100 mL volume). Then, humidified N_2 gas was purged into the flask for 1.5 h at 25 °C. IHP was added to block the competing reactions with the β subunits of HbA. Subsequently, DBBF (2.5 mg, [DBBF]/[HbA] = 1.25, mol/mol) was added to the mixture. The resultant was stirred for another 2 h under N_2 atmosphere at 37 °C. Then, an aqueous solution of glycine (1.5 M, 0.625 mL) was added to the solution to terminate the reaction. The mixture was stirred for 2 h. After the CO gas

flowed into the flask, the reactant was loaded for GFC performed using a Sephadex G25 (superfine) column to eliminate the unreacted DBBF, thereby generating ααHbA(T).

The PBS solution of oxy ααHbA(T) (0.1 mM, 20 mL) in a round-bottom flask (100 mL volume) was purged with a stream of humidified N_2 for 2 h at 25 °C. From this step, all the reactions were performed under N_2 atmosphere. A DMSO solution of SMCC (20 mM, 2.0 mL) was added dropwise to the obtained deoxy ααHbA(T) solution. Then the mixture was stirred for 2 h at 25 °C. Next, the PBS solution of glycine (1.5 M, 0.27 mL) was added to the solution using a humidified N_2 gas stream, followed by stirring for 2 h at 25 °C. Finally, the reactant was added to the HSA solution (2.0 mM, 40 mL in PBS) using an N_2 stream. It was stirred gently in the dark for 14 h at 25 °C. The resultant was subjected to GFC (Superdex 200 pg in XK50/60 column) using PBS (pH 7.4, 50 mM) as the running buffer. We collected all the clusters without HSA. Using the total protein and Hb assays, the average HSA/HbA ratio of the obtained clusters was found to be 3.0 ± 0.2, which is denoted as ααHbA(T)–HSA_3.

3. Results and discussion

3.1. Synthesis of HbA–HSA_m clusters

HSA comprises three homologous domains (I–III), each of which consists of A and B subdomains.[32,33] This heart-shaped protein includes a total of 35 Cys residues, whereby 17 pairs of the residues form intramolecular disulphide bonds. The results show that only one free Cys in reduced form remains at position 34. It allows for site-specific binding. A heterobifunctional cross-linker, succinimidyl-4-(*N*-maleimidomethyl)cyclohexane-1-carboxylate (SMCC), was used as a connector between the particular Cys-34 of HSA and the surface Lys groups of HbA to create a core–shell cluster with HbA in the centre and HSA at the periphery (HbA–HSA_m, Fig. 1).

First, SMCC was reacted with carbonyl HbA in PBS (pH 7.4). Then, the binding number of SMCC on HbA was 6.1 per molecule, as ascertained from the maleimide assay. The obtained SMCC–HbA was added dropwise to the HSA solution, followed by stirring for 14 h. The examination of the reaction mixture using SEC revealed four peaks in the high molecular weight region (Fig. 2A, elution time 14–19 min). Native-PAGE also revealed three new bands above HSA (Fig. 2B). The major products (bands I–III) were isolated using gel filtration chromatography (GFC) (Fig. 2A). Based on the Hb and protein assays, the HSA/HbA ratios were determined as 1.9, 3.0, and 3.9 for the band-I, -II, and -III compounds, respectively. We identified these clusters respectively as HbA–HSA_2 (heterotrimer), HbA–HSA_3 (heterotetramer), and HbA–HSA_4 (heteropentamer) (Fig. 1). The formation ratios of the heterotrimer, heterotetramer, and heteropentamer were estimated as 25%, 45%, and 24% from curve fitting of the SEC profile. The HbA–HSA_1 (heterodimer) was also formed and observed at 18.3 min in the SEC curve. It is consistent with our previous result on HbBv–HSA_m.[19] However, HbA–HSA_1 with a low formation ratio was not detected in the native-PAGE,

This journal is © The Royal Society of Chemistry 2015

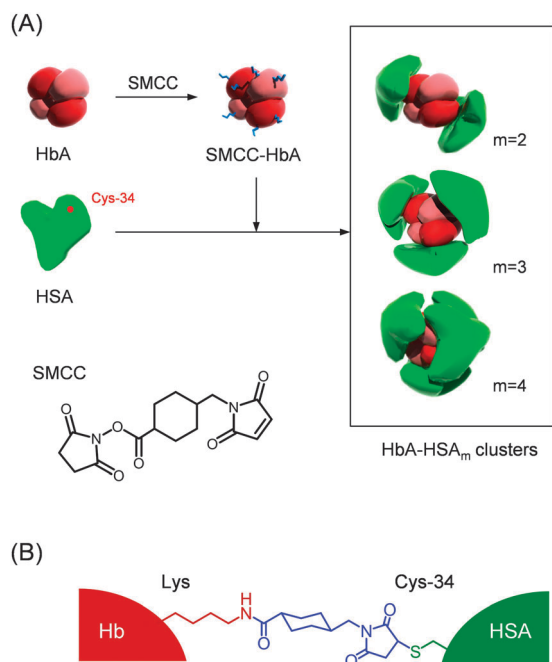*J. Mater. Chem. B*, 2015, **3**, 6157–6164 | 6159

Fig. 1 (A) Schematic illustration of the synthetic route of HbA–HSA$_m$ clusters using heterobifunctional cross-linkers (SMCC). (B) The covalent linkage structure between the Lys residue of HbA and the Cys-34 residue of HSA.

Fig. 2 (A) SEC profiles of the reaction mixture of HbA and HSA (black dotted line), purified HbA–HSA$_4$ (green line), HbA–HSA$_3$ (red line), HbA–HSA$_2$ (blue line), and the cluster mixture HbA–HSA$_3$ (purple line). (B) The native–PAGE results of the same samples: I, HbA–HSA$_2$; II, HbA–HSA$_3$; III, HbA–HSA$_4$.

because of the differences in the limit of detection and dynamic range of SEC and PAGE analysis.

In different preparations, we collected all the products together using GFC and removed the unreacted HSA. This cluster mixture, indicated as HbA–HSA$_3$ with italicized subscript 3, showed an HSA/HbA ratio of 3.0 ± 0.2 on average.

Unlike HbBv having only a single Cys at the 93 position of the β subunit,[34] human HbA possesses three Cys residues at 93(β), 104(α), and 112(β) (a total of six Cys residues per molecule).[35] Then the SMCC–HbA might form unfavourable HbA oligomers *via* intermolecular connections between their maleimide terminals and cysteinyl thiols in different HbA. Nonetheless, such oligomerization did not occur because Cys-104(α) and Cys-112(β) are known to be non-reactive sites.[36] The remaining Cys-93(β) is located in hydrophobic crevices of the protein, at least 15 Å deep with respect to the molecular surface.[35] The maleimide arm of SMCC–HbA (10 Å spacer length) is too short to bind Cys-93(β) of different HbA. Moreover, sulphydryl group of Cys-93(β) in HbA was masked by the maleimide-end of free SMCC (described below). We concluded that SMCC is an excellent cross-linker to create structurally defined core–shell HbA–HSA$_m$ clusters.

The CD spectrum of HbA–HSA$_3$ clusters coincided well with the sum of the HbA spectrum and a three-fold enlarged HSA spectrum (Fig. 3), which implies that (i) the HbA : HSA composition ratio is 1 : 3 (mol : mol) and that (ii) the secondary structure of the individual protein unit remains unaltered after the cluster formation. The HbA–HSA$_2$ and HbA–HSA$_4$ clusters showed CD spectra with HbA + 2HSA and HbA + 4HSA,
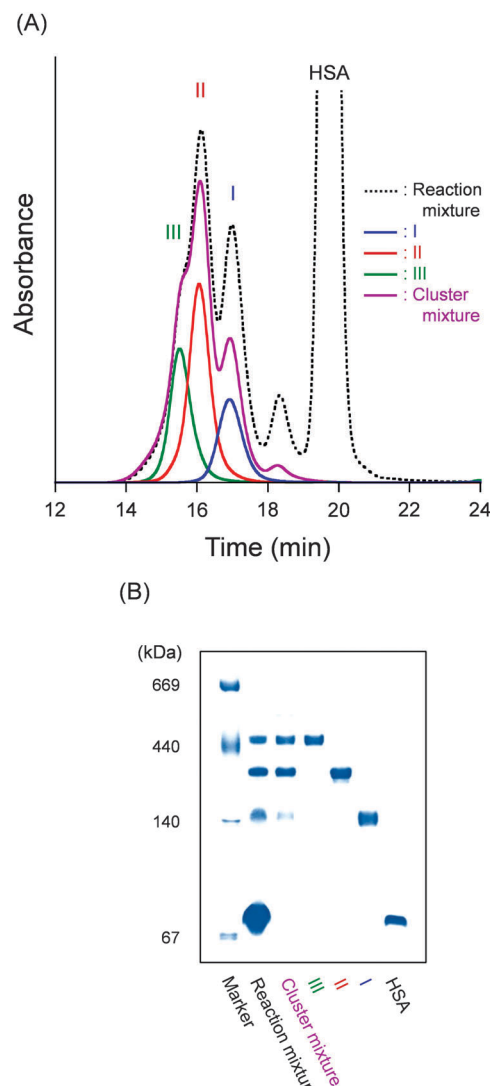
indicating that the respective HbA : HSA ratios are 1 : 2 and 1 : 4 (mol : mol) (Fig. 3).

The diameters of HbA–HSA$_m$ clusters observed by dynamic light scattering (DLS) measurements increased gradually with the number of HSA units: 7.6 nm for HbA–HSA$_2$, 8.9 nm for HbA–HSA$_3$, and 10.2 nm for HbA–HSA$_4$ (Fig. S1, ESI†). Their isoelectric points (pI: 5.0–5.2) were all significantly lower than the value of native HbA (pI: 7.0) and were very close to that of HSA (pI: 4.9) (Fig. S2, ESI†). These results supported that the HbA core is wrapped covalently by HSA. The surface net charges of the HbA–HSA$_m$ clusters are reasonably negative to circulate in the bloodstream for a long time. The mixture of clusters, HbA–HSA$_3$, also demonstrated the same CD spectrum, diameter (8.9 nm), and pI value (5.1) as the HbA–HSA$_3$ tetramer (Fig. 3 and Fig. S1 and Table S1, ESI†).
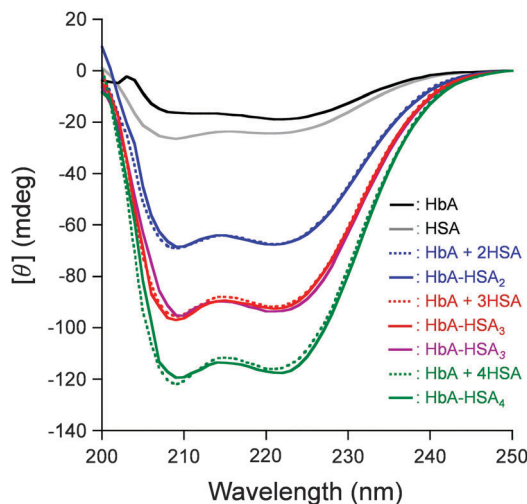
Fig. 3   CD spectra of HbA–HSA$_m$ (m = 2, 3, 4), HbA–HSA$_3$, HbA, and HSA (0.2 μM) in PBS solution (pH 7.4) at 25 °C.

3.2.   Structure analysis of HbA–HSA$_3$ clusters

TEM observations of the negatively stained sample of HbA–HSA$_3$ clusters showed individual particles with a diameter of approximately 10 nm. The detailed structure information was unobtainable from the raw images because of the low contrast and the small size of the clusters. We used additional image processing procedures (single-particle analysis), such as alignment, multivariate statistical analysis, and classification procedures, to produce class sum images with an enhanced signal-to-noise ratio.[19,26–29] From the obtained class sum images (Fig. 4A), the 3D volume of the HbA–HSA$_3$ clusters was reconstructed using the angular reconstitution technique. Later, we calculated a presentation of the two protein constituents by fitting their PDB-data into the reconstructed framework. The fitting of three HSAs defined the spatial arrangement of Cys-34, which revealed
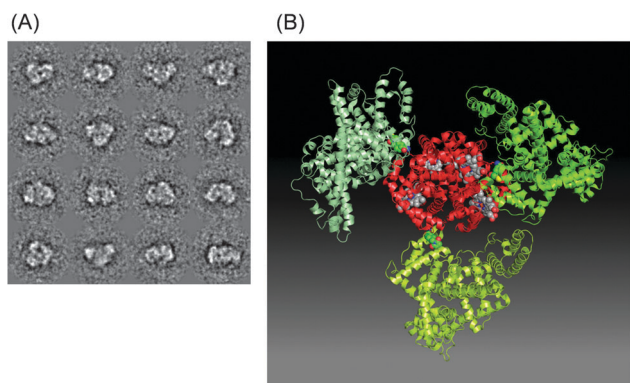
the potential binding Lys partners of the HbA sphere. The examination of the structural geometry revealed four (two sets) possible conformers of the HbA–HSA$_3$ clusters. Each has three Lys binding sites on the HbA surface for HSA. Based on our assumption that the three Lys groups (HSA binding sites) on HbA maintain some mutual separation because of the electrostatic repulsion between the conjugated HSA moieties, we reasoned that one variant is the most probable conformer, having binding sites of Lys-90(α_1), Lys-82(β_1), and Lys-90(α_2). The final detailed structure of HbA–HSA$_3$ clusters is portrayed in Fig. 4B and Movie S1 (ESI†). Remarkably, the HSA binding sites on HbA closely resemble those of HbBv–HSA$_3$ clusters [Lys-90(α_1), Lys-82(β_1), and Lys-16(α_2)],[19] but they are not identical. In the case of human HbA, Lys-90(α_2) is the binding partner instead of Lys-16(α_2) in HbBv.

3.3.   O$_2$-binding properties of HbA–HSA$_m$

The visible absorption spectra of the HbA–HSA$_m$ clusters in PBS solution under N$_2$, O$_2$, and CO atmospheres (deoxy, oxy, and carbonyl forms, respectively) were almost identical to the corresponding spectra of the naked HbA (Fig. 5, Table S2, ESI†).[37] We infer that the electronic states of the hemes in HbA were unaffected by the covalent linkages of HSA.

The O$_2$ affinity (P_{50}: O$_2$-partial pressure where Hb is half-saturated with O$_2$) and the co-operativity coefficient (Hill coefficient, n) of the HbA–HSA$_m$ clusters can be measured using an automatic recording system for the blood O$_2$-equilibrium curve: a Hemox Analyzer. The P_{50} of native HbA was ascertained as 12 Torr at 37 °C,[9,38] whereas the value of HbA–HSA$_3$ was 8 Torr (Table 1). Apparently, the HbA–HSA$_3$ clusters show a higher O$_2$-affinity than HbA. The n value decreased from 2.4 to 1.4. Equivalent P_{50} and n reductions were also observed in HbA–HSA$_2$ and HbA–HSA$_4$ clusters (P_{50} = 8–9 Torr) (Table 1). No clear dependence of these parameters on the HSA-binding number (m = 2, 3, 4) was found. Two possible explanations exist for the increase of O$_2$ affinity and the decrease in co-operativity. The first is the binding of the maleimide
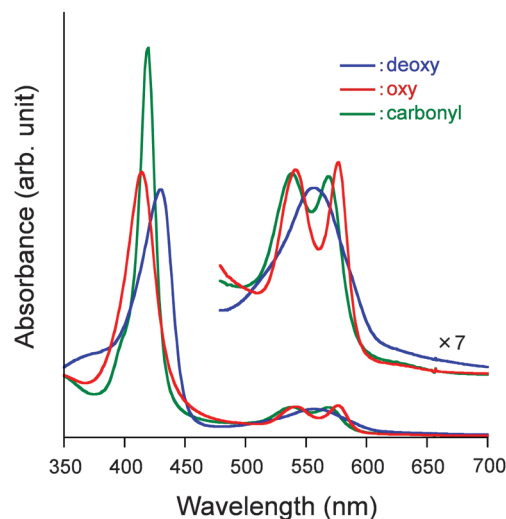

Fig. 4   (A) Gallery of a selected class sum images representing different spatial orientations of HbA–HSA$_3$ clusters. (B) The spatial molecular view of HbA–HSA$_3$ clusters derived from a 3D volume reconstruction calculated from a set of class sum images. Color code: HbA, red; HSAs, chartreuse, lemon, and pale green. Hemes (C, grey) in HbA, Cys-34 (S, yellow) in HSA, and crosslinking moieties (C, green) are shown in space-filling representations. PDB ID: 2DN3 for HbA, 1E78 for HSA. Movie, attached wmv file (Movie S1, ESI†).

Fig. 5   Visible absorption spectral changes of the HbA–HSA$_3$ clusters in PBS solution (pH 7.4) at 25 °C.

Table 1 O_2-binding parameters of HbA–HSA$_m$ clusters in PBS solution (pH 7.4) at 37 °C

	P_{50} (Torr)	n
HbA–HSA$_2$	8	1.4
HbA–HSA$_3$	8	1.4
HbA–HSA$_4$	9	1.4
HbA–HSA$_3$	8	1.4
HbA(T)–HSA$_3$	26	1.2
$\alpha\alpha$HbA(T)–HSA$_3$	35	1.4
HbA	12	2.4
	12[a]	2.4[a]
	15[b]	2.3[b]
RBC	25	2.5

[a] In Hemox buffer (pH 7.4), 37 °C.[38] [b] In PBS (pH 7.4), 37 °C.[9]

terminal of free SMCC to the thiol group of Cys-93(β) (Fig. 6A, upper) in HbA. Modification of Cys-93(β), which is adjacent to the proximal histidine [His-92(β)] coordinated to the prosthetic heme group,[35] is known to increase the O_2 affinity.[9,10,13,19] Furthermore, it reduces the available motion of the $\alpha_1\beta_1/\alpha_2\beta_2$ interface and thereby induces disturbance in the quaternary structure of HbA from the T-state to the R-state.[13] As described above, HbA includes a total of six Cys residues in the tetramer units, but only Cys-93(β) shows high reactivity in the oxy or carbonyl form.[36] In fact, the number of active cysteinyl thiols per HbA decreased from 2.0 to 0.2 after the SMCC reaction,[25,39] implying that two Cys-93(β) of HbA are likely to be masked by SMCC maleimide. Fortunately, no Lys residue reacts with the opposite side of the SMCC bound Cys-93(β). The second reason is the modification of surface Lys groups of HbA by the succinimide terminal of SMCC (Fig. 6B). It is necessary to create the clusters, but the chemical modification of Lys groups on HbA influences the O_2 affinity and decreases the Hill coefficient.[5,8,40] Particularly, Lys-82(β) plays a key role in

controlling the quaternary structural change from the T-state to R-state. Our image processing and 3D reconstruction demonstrated that Lys-82(β) is a binding partner of Cys-34 of HSA, as described earlier. Overall, it can be concluded that the blocking of Cys-93(β) increases the O_2 affinity. Modification of surface Lys groups locks the R-state conformation of the central HbA, resulting in the decrease of the O_2-binding co-operativity.

3.4. O_2-binding properties of HbA(T)–HSA$_3$ and $\alpha\alpha$HbA(T)–HSA$_3$ clusters

The heterobifunctional cross-linker SMCC binds not only to the reactive amino groups of Lys on HbA, but also to the thiol group of Cys-93(β). Consequently, the clusters showed high O_2-affinity. In our synthesis, the central HbA is always maintained in the carbonyl form to prevent the autoxidation of the ferrous hemes. In deoxygenated T-state HbA (deoxy form), Cys-93(β) is less accessible to modifying agents (Fig. 6A, lower).[36] If all the synthetic reactions using deoxy HbA are performed in N_2, then SMCC cannot bind to the sulphydryl group of Cys-93(β). Therefore, a different type of HbA–HSA$_m$ clusters with low O_2-affinity might be conferred. For this reason, the HbA–HSA$_m$ clusters were prepared under N_2 atmosphere. After the reaction of SMCC with deoxy HbA, a large excess amount of glycine was added to quench the succinimide group of the unreacted cross-linker. Subsequently, the mixture was reacted with HSA for 14 h. The resultant was subjected to GFC. All the major products were collected together as HbA(T)–HSA$_3$ (HSA/HbA ratio = 2.9 ± 0.2 on average). The physicochemical properties of HbA(T)–HSA$_3$ clusters were identical to those observed for HbA–HSA$_3$ (Table S1, ESI†).

As expected, the obtained clusters showed a markedly lower O_2-affinity (P_{50} = 26 Torr) than the native HbA (12 Torr) (Table 1). The thiol assay of the molecule revealed that Cys-93(β) residues of the HbA core remained in reduced form. By preventing SMCC maleimide from accessing Cys-93(β), we were able to produce HbA(T)–HSA$_3$ clusters with a low O_2-affinity, which nevertheless resembles that of human RBC (P_{50} = 25 Torr). The n value of the HbA(T)–HSA$_3$ clusters was 1.2, indicating a loss of O_2-binding co-operativity. We inferred that the HbA centre was locked in the T-state conformation by the binding of SMCC to surface Lys groups on HbA under N_2 atmosphere. Low P_{50} and n of the SMCC-modified HbA(T) intermediate (27 Torr, 1.3) proved this hypothesis and showed that HSA wrapping did not affect the O_2-binding equilibrium of the core HbA.

Other Hb-derivative-containing clusters were designed to decrease the O_2 affinity further. HbA cross-linked between the α-subunits of Walder et al. was a pioneering product generated by the reaction of bis(3,5-dibromosalicyl)fumarate (DBBF) with deoxy HbA.[30,31] The X-ray crystallographic studies revealed a cross-linking bridge between Lys-99(α_1) and Lys-99(α_2). The reaction of DBBF at Lys-99(α) is very specific for the deoxy quaternary structure (T-state); the obtained $\alpha\alpha$HbA(T) showed a low O_2-affinity (P_{50} = 31–33 Torr).[10,18] It is particularly noteworthy that this cross-linking does not invoke the reduction of O_2-binding co-operativity (n = 2.4–2.5). Therefore, we used $\alpha\alpha$HbA(T) as the core of the clusters. Using $\alpha\alpha$HbA(T),
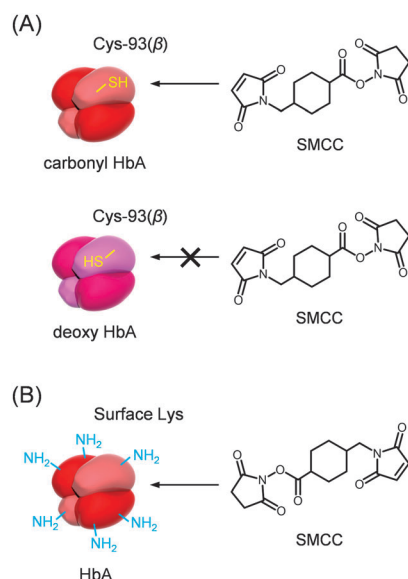

Fig. 6 (A) Binding of the maleimide terminal of SMCC to the thiol group of Cys-93(β) in HbA. (B) Binding of the succinimide terminal of SMCC to surface Lys groups of HbA.

6162 | J. Mater. Chem. B, 2015, **3**, 6157–6164

This journal is © The Royal Society of Chemistry 2015

the corresponding cluster, ααHbA(T)–HSA$_3$, was synthesized under N_2 atmosphere using the same procedure as that used for HbA(T)–HSA$_3$. The physicochemical properties of ααHbA(T)–HSA$_3$ (average HSA/HbA ratio = 3.0 ± 0.2) were comparable to those of HbA–HSA$_3$ (Table S1, ESI†).

The ααHbA(T)–HSA$_3$ clusters showed a markedly low O_2-affinity (P_{50} = 35 Torr): lower than that of human RBC (Table 1). This low affinity is attributable to two facts: (i) the Lys-99(α_1) and Lys-99(α_2) residues were cross-linked intra-molecularly. (ii) The Cys-93(β) residue of the ααHbA(T) core was not masked by SMCC. However, the n value of ααHbA(T)–HSA$_3$ was low: 1.4. We inferred that the T-state conformation of the ααHbA(T) core was preserved by chemical modification of the surface Lys groups.

4. Conclusions

Covalent enfolding of human HbA by HSA using SMCC generates structure-defined core–shell protein clusters. The major product is a HbA–HSA$_3$ heterotetramer. The negative surface net charge (pI: 5.0–5.2) supports the enwrapping of HbA by HSA. It can be beneficial in applications as a potential O_2-carrier. Based on image processing of the TEM data and 3D reconstruction procedures, the complete triangular structure of the core–shell HbA–HSA$_3$ clusters was ascertained. Volume fitting of the molecular constituents enabled us to assign a putative spatial arrangement of HbA and HSAs. The O_2 affinity of HbA–HSA$_m$ became higher (P_{50} = 8–9 Torr) than that of the native HbA because the Cys-93(β) residue in HbA reacted with the maleimide terminal of SMCC. In the T-state (deoxy) HbA, Cys-93 is non-accessible to the reagent. Due to this reason, SMCC cannot bind to the cysteinyl thiol group. Consequently, the preparation of the HbA(T)–HSA$_3$ clusters under N_2 atmosphere caused a useful reduction in the O_2 affinity, yielding a P_{50} value of 26 Torr, which closely approximates that of human RBC. The ααHbA(T)–HSA$_3$ clusters showed a markedly low O_2-affinity (P_{50} = 35 Torr). We prepared three HbA–HSA$_m$ clusters showing different P_{50} values of 8, 26, and 35 Torr. Our results imply that the O_2 affinity of the HbA–HSA$_m$ clusters can be modulated by altering the conformational state of the HbA centre. These clusters with controllable O_2-affinities can support a new generation of RBC substitutes, which are better tuned to play a role in O_2 transport. They can be of great medical importance as alternative materials for human RBC transfusion in various clinical settings.

Acknowledgements

Notes and references

1 J. E. Squires, *Science*, 2002, **295**, 1002–1005.
2 J. S. Jahr, A. Sadighi, L. Doherty, A. Li and H. W. Kim, in *Chemistry and Biochemistry of Oxygen Therapeutics: From Transfusion to Artificial Blood*, ed. S. Bettati and A. Mozzarelli, John Wiley & Sons, West Sussex, 2011, pp. 301–316.
3 R. Kluger and F. E. Lui, in *Hemoglobin-Based Oxygen Carriers as Red Cell Substitutes and Oxygen Therapeutics*, ed. H. W. Kim and A. G. Greenburg, Springer-Verlag, Berlin Heidelberg, 2013, pp. 159–183.
4 C. L. Mondery-Pawlowski, L. L. Tian, V. Pan and A. S. Gupta, *Biomacromolecules*, 2013, **14**, 939–948.
5 R. Kluger and J. Zhang, *J. Am. Chem. Soc.*, 2003, **125**, 6070–6071.
6 P. W. Buehler, R. A. Boykins, Y. Jia, S. Norris, D. I. Freedberg and A. I. Alayash, *Anal. Chem.*, 2005, **77**, 3466–3478.
7 L. B. Pearce, M. S. Gawryl, V. T. Rentko, P. F. Moon-Massat and C. W. Rausch, in *Blood Substitutes*, ed. R. M. Winslow, Elsevier, San Diego, 2006, pp. 437–450.
8 K. D. Vandegriff, A. Malavalli, J. Wooldbridge, W. Lohman and R. M. Winslow, *Transfusion*, 2003, **43**, 509–516.
9 B. M. Manjula, A. G. Tsai, R. Upadhya, K. Perumalsamy, P. K. Smith, A. Malavalli, K. Vandegriff, R. M. Winslow, M. Intaglietta, M. Prabhakaran, J. M. Friedman and A. S. Acharya, *Bioconjugate Chem.*, 2003, **14**, 464–472.
10 D. Li, T. Hu, B. N. Manjula and S. A. Acharya, *Bioconjugate Chem.*, 2009, **20**, 2062–2070.
11 F. D'Agnilloo and T. M. S. Chang, *Nat. Biotechnol.*, 1998, **16**, 667–671.
12 A. Alagic, A. Koprianiuk and R. Kluger, *J. Am. Chem. Soc.*, 2005, **127**, 8036–8043.
13 Y. Zhang, V. S. Bhatt, G. Sun, P. G. Wang and A. F. Palmer, *Bioconjugate Chem.*, 2008, **19**, 2221–2230.
14 C. Natanson, S. J. Kern, P. Lurie, S. M. Banks and S. M. Wolfe, *J. Am. Med. Assoc.*, 2008, **299**, 2304–2312.
15 R. Kluger, *Curr. Opin. Chem. Biol.*, 2010, **14**, 538–543.
16 S. C. Shultz, B. Grady, F. Cole, I. Hamilton, K. Burhop and D. S. Malcolm, *J. Lab. Clin. Med.*, 1993, **122**, 301–308.
17 D. H. Doherty, M. P. Doyle, S. R. Curry, R. J. Vali, T. J. Fattor, J. S. Olson and D. D. Lemon, *Nat. Biotechnol.*, 1998, **16**, 672–676.
18 R. J. Rohlfs, E. Bruner, A. Chiu, M. L. Gonzaless, D. Magde, M. D. Magde Jr., K. D. Vandegriff and R. M. Winslow, *J. Biol. Chem.*, 1998, **273**, 12128–12134.
19 D. Tomita, T. Kimura, H. Hosaka, Y. Daijima, R. Haruki, K. Ludwig, C. Böttcher and T. Komatsu, *Biomacromolecules*, 2013, **14**, 1816–1825.
20 H. Hosaka, R. Haruki, K. Yamada, C. Böttcher and T. Komatsu, *PLoS One*, 2014, **9**, e110541.
21 Y. Daijima and T. Komatsu, *Chem. Commun.*, 2014, **50**, 14716–14719.
22 T. Peters, *All about Albumin: Biochemistry, Genetics and Medical Applications*, Academic Press, San Diego, CA, 1996.
23 C. C. Michel, *Cardiovasc. Res.*, 1996, **32**, 644–653.
24 M. F. Perutz, G. Fermi, C. Poyart, J. Pagnier and J. Kister, *J. Mol. Biol.*, 1993, **233**, 536–545.

This journal is © The Royal Society of Chemistry 2015

J. Mater. Chem. B, 2015, **3**, 6157–6164 | **6163**

25 D. R. Grassetti and J. F. Murray Jr., *Arch. Biochem. Biophys.*, 1967, **119**, 41–49.

26 M. Kellermann, W. Bauer, A. Hirsch, B. Shade, K. Ludwig and C. Böttcher, *Angew. Chem., Int. Ed.*, 2004, **43**, 2959–2962.

27 B. Trappmann, K. Ludwig, M. R. Radowski, A. Shukla, A. Mohr, H. Rehage, C. Böttcher and R. Haag, *J. Am. Chem. Soc.*, 2010, **132**, 11119–11124.

28 M. van Heel, G. Harauz, E. V. Orlova, R. Schmidt and M. Schatz, *J. Struct. Biol.*, 1996, **116**, 17–24.

29 E. V. Orlova, P. Dube, J. R. Harris, E. Beckman, F. Zemlin, J. Markl and M. van Heel, *J. Mol. Biol.*, 1997, **271**, 417–437.

30 S. R. Snyder, E. V. Welty, R. Y. Walder, L. A. Williams and J. A. Walder, *Proc. Natl. Acad. Sci. U. S. A.*, 1987, **84**, 7280–7284.

31 R. Y. Walder, M. E. Andracki and J. A. Walder, *Methods Enzymol.*, 1994, **231**, 274–280.

32 S. Curry, H. Madelkow, P. Brick and N. Franks, *Nat. Struct. Biol.*, 1998, **5**, 827–835.

33 A. A. Bhattacharya, S. Curry and N. P. Frank, *J. Biol. Chem.*, 2000, **275**, 38731–38738.

34 T. C. Mueser, P. H. Roger and A. Arnone, *Biochemistry*, 2000, **39**, 15353–15364.

35 S.-Y. Park, T. Yokoyama, N. Shinbayama, Y. Shiro and J. R. Tame, *J. Mol. Biol.*, 2006, **360**, 690–701.

36 P. W. Buehler, R. A. Boykins, S. Norris and A. L. Alayash, *Anal. Chem.*, 2006, **78**, 4634–4641.

37 E. Antonini and M. Brunori, Hemoglobin and Myoglobin in Their Reactions with Ligandsin *North-Holland Research Monographs. Frontiers of Biology*, ed. A. Neuberger and E. L. Tatum, North-Holland Pub. Co., Amsterdam, vol. 21, 1971, pp. 13–39.

38 J. Elmer, K. Zorc, S. Rameez, Y. Zhou, P. Cabrales and A. F. Palmer, *Transfusion*, 2012, **52**, 1729–1740.

39 Non-reactive cysteinyl thiol groups of Cys-104(α) and Cys-112(β) of HbA cannot be detected by the general thiol assay using 4,4′-dithiopyridine.

40 D. Hu and R. A. Kluger, *Biochemistry*, 2008, **47**, 12551–12561.

6164 | *J. Mater. Chem. B*, 2015, **3**, 6157–6164

This journal is © The Royal Society of Chemistry 2015